



**HAL**  
open science

## High-Resolution Wavenumber Analysis (HRWA) for the mechanical characterization of viscoelastic beams

Pierre Margerit, Arthur Lebée, Jean-François Caron, Xavier Boutillon

### ► To cite this version:

Pierre Margerit, Arthur Lebée, Jean-François Caron, Xavier Boutillon. High-Resolution Wavenumber Analysis (HRWA) for the mechanical characterization of viscoelastic beams. *Journal of Sound and Vibration*, 2018, 443, pp.198-211. 10.1016/j.jsv.2018.06.062 . hal-01825733

**HAL Id: hal-01825733**

**<https://hal.science/hal-01825733v1>**

Submitted on 22 Jun 2019

**HAL** is a multi-disciplinary open access archive for the deposit and dissemination of scientific research documents, whether they are published or not. The documents may come from teaching and research institutions in France or abroad, or from public or private research centers.

L'archive ouverte pluridisciplinaire **HAL**, est destinée au dépôt et à la diffusion de documents scientifiques de niveau recherche, publiés ou non, émanant des établissements d'enseignement et de recherche français ou étrangers, des laboratoires publics ou privés.

# High Resolution Wavenumber Analysis (HRWA) for the Mechanical Characterisation of Viscoelastic Beams

Pierre Margerit<sup>a</sup>, Arthur Lebé<sup>a,\*</sup>, Jean-François Caron<sup>a</sup>, Xavier Boutillon<sup>b</sup>

<sup>a</sup>Laboratoire Navier, UMR 8205, École des Ponts, IFSTTAR, CNRS, UPE, Champs-sur-Marne, France

<sup>b</sup>Laboratory of Solid Mechanics (LMS), École polytechnique, Palaiseau, France

---

## Abstract

The High-Resolution Wavenumber Analysis (HRWA) is presented. It identifies complex wavenumbers and amplitudes of waves composing the harmonic response of a beam. Based on the frequency dependence of these wavenumbers, experimental dispersion branches corresponding to various beam motions (e.g bending, torsion) can be retrieved. The HRWA method is compared to the *Mc Daniel* and the *Inverse Wave Correlation (IWC)* methods. It overcomes some drawbacks of these methods: the wavenumber resolution is enhanced. Also, the wavenumber search problem is expressed as a linear problem, making the method computationally efficient. A number of wavenumbers can be identified automatically, thanks to a statistical criterion. First, the noise sensitivity of each method is investigated in the basis of synthesised measurements. For this criterion, the HRWA and *Mc Daniel method* performances are close and much better than *IWC*. Moreover, the HRWA is five to twenty times faster to compute than other methods, depending on the mesh size. Second, an experimental case is presented where bending and torsion waves are identified, yielding an apparent viscoelastic Young and shear moduli on a wide-frequency range.

*Keywords:* Structure identification, Non-destructive testing, Signal Processing, Wavenumber extraction

---

## 1. Introduction

With the apparition of full-field contactless measurement devices (e.g. scanning doppler laser vibrometers or high-speed cameras), displacement or velocity measurements can be performed on fine meshes, with a large number of points. Thanks to this major improvement, non-destructive structural characterisation methods have been developed [1, 2, 3, 4]. Some of them focus on the identification of structural waves in the *medium frequency* domain [5, 6, 7, 8, 9]. These methods aim at filling the gap between low-frequency methods, (*Oberst* [10, 11], modal analysis [12, 13, 14, 15, 16] or Dynamical Mechanical Analysis (DMA) [17]) and ultrasonic testing [18, 19, 20].

---

\*Corresponding author. [arthur.lebee@enpc.fr](mailto:arthur.lebee@enpc.fr)

The present work focuses on applications to beam, considered as waveguides. Waves travelling in these structures are representative of the beam section motions: for example bending, twist or longitudinal motion. In these unidimensionnal structures, the wavenumbers are characteristic of the local structural behaviour: far from singularities, boundary conditions and sources have an influence on the wave amplitudes only. These wavenumbers are given by reduced beam models (e.g. Euler or Timoshenko models) or more elaborated schemes like Wave Finite elements [21]. The experimentally extracted wavenumbers can be used to identify apparent viscoelastic parameters of reduced models via an inverse problem [9].

The existing Mc Daniel [7] and IWC [5, 6] (Inhomogeneous Wave Correlation) methods are two candidate for the extraction of waves in the harmonic response of beams. However, these methods have some drawbacks (i) in low frequency, the Fourier based IWC method suffers from resolution limitations; (ii) in practice, the beam response is composed of multiple wave types (e.g. twist, compression, shear) and both existing methods fail to separate the different wave contributions, as they postulate the number of waves present in the signal; (iii) the formulation of these methods leads to a computationally expensive non-linear problem that has to be solved, with a complex wavenumber as parameter.

The aim of the High Resolution Wavenumber Analysis (HRWA) presented in this paper is to overcome the limitations of the existing wavenumber extraction techniques. It makes use of the subspace-based identification algorithm ESPRIT [22] (*Estimation of Signal Parameters via Rotational Invariance Techniques*). Subspace-based methods are widely-used in linear system identification, using for example the state-variable framework [23, 24]. Another example is the ERA [25] (*Eigenvalue Realisation Algorithm*), which is devoted to the identification of the modal parameters of a measured system. Thanks to the use of the ESPRIT algorithm, some limitations of the Mc Daniel and IWC methods are overcome: (i) the algorithm resolution is high, as it uses a recurrence property of the signal to identify the wave parameters; (ii) by using the subspace decomposition, the number of waves contained in the signal can be estimated automatically with the ESTER criterion [26]; (iii) the complex wavenumbers are the solution of an optimisation-free problem thus the computational cost is lightened.

With the HRWA, a discrete number of complex wavenumbers is identified in the harmonic response of a beam with a high resolution. Based on the dependence of the extracted wavenumbers on frequency, experimental dispersion branches are retrieved. From these branches are identified the beam viscoelastic properties. Thanks to the high resolution aspects of the HRWA, the low-frequency limit of wavenumber extraction is lowered. Also, with the automated identification of multiple wavenumbers, strain mechanisms can be well separated, extending the upper frequency limit.

The paper is organised as follows. Firstly, theoretical wavenumbers are derived from the Euler and the Timoshenko beam models. The ability to identify beam properties from the wavenumbers is illustrated. Then, a common framework of wavenumber extraction methods is given, and the existing IWC method and McDaniel method reformulated in this framework. Secondly, the HRWA is developed in details. A summary of the algorithm is given, that allows to identify viscoelastic properties of the beam. Thirdly, a numerical

study based on synthesised harmonic responses of an Euler beam in bending motion only is developed, where the Mc Daniel method is taken as reference. The Mc Daniel method, IWC method and the proposed HRWA are compared in terms of sensitivity to noise ratio and computation time. Finally, an experimental result is given on the simultaneous identification of frequency-dependent apparent viscoelastic Young and shear modulus, for both beam models.

## 2. Natural wavenumbers in a beam

All along the paper, the beam section is considered as homogeneous and made of a linear viscoelastic isotropic material with density  $\rho$ , Young modulus  $E$  and shear modulus  $G$ . However, the present method is applicable to higher-order beam models and more complex material configurations. The axis and the geometry of the beam are presented in Fig. 1 ( $x$  being the beam's direction). Not considering the bending motion along  $y$ , the beam neutral axis is assumed to remain in the  $(O, x, z)$  plane.

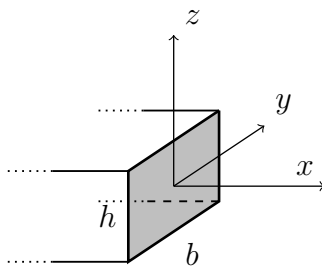


Figure 1: Beam geometry and coordinate axis

### 2.1. The Euler model

For the sake of simplicity, the Euler beam model is used for the numerical case considered in this paper. The linearised displacement field  $u$  is given by:

$$\mathbf{u}(x, y, z, t) = V(x, t) \mathbf{e}_x + W(x, t) \mathbf{e}_z - z W'(x, t) \mathbf{e}_x + \Theta(x, t) (y \mathbf{e}_z - z \mathbf{e}_y) \quad (1)$$

where  $V$  and  $W$  are respectively the longitudinal and transverse displacements,  $\Theta$  is the rotation angle of the beam section with respect to the  $x$  axis, and  $\bullet'$  denotes the partial derivative with respect to  $x$ .

Along the paper, the harmonic dependence on time of real physical quantities is accounted for by making them complex according to the  $e^{i\omega t}$  convention (where  $i$  denotes the imaginary unit). The local harmonic response of the beam at the angular frequency  $\omega$  (except on sources or at boundaries locations) obeys the following uncoupled linear homogeneous equations:

$$E V'' = -\omega^2 \rho V \quad (2a)$$

$$I_b E W'''' = -\omega^2 M W \quad (2b)$$

$$I_t G \Theta'' = -\omega^2 J \Theta \quad (2c)$$

with  $A = bh$ ,  $I_b = bh^3/12$ ,  $J = \rho(bh^3 + hb^3)/12$ ,  $I_t = \kappa J/\rho$ ,  $M = \rho A$  and  $\kappa$  being a correction factor for twist inertia momentum, related to the shape of the beam's section.

By taking exponential solutions as function of  $x$ , the displacement components are expressed as a sum of the solutions of the previous equations:

$$V(x) = v_1 e^{ik_v x} + v_2 e^{-ik_v x} \quad (3a)$$

$$W(x) = w_1 e^{ik_b x} + w_2 e^{-ik_b x} + w_3 e^{k_b x} + w_4 e^{-k_b x} \quad (3b)$$

$$\Theta(x) = \theta_1 e^{ik_t x} + \theta_2 e^{-ik_t x} \quad (3c)$$

where the wave amplitudes  $v_r$ ,  $w_r$  and  $\theta_r$  are given by boundary conditions.

According to the  $e^{i\omega t}$  convention specified above, the  $e^{-ikx}$  waves are forward-propagating waves. The three following dispersion laws are obtained:

$$k_v^2 = \omega^2 \frac{\rho}{E} \quad , \quad k_b^4 = \omega^2 \frac{M}{EI_b} \quad \text{and} \quad k_t^2 = \omega^2 \frac{J}{GI_t} \quad (4)$$

It is of common practice to account for the viscoelastic behaviour of the material by taking complex moduli  $\mathbf{E} = E(1 + i\eta_E)$  and  $\mathbf{G} = G(1 + i\eta_G)$  with positive (and small) imaginary parts, according to the  $e^{i\omega t}$  convention. The wavenumbers become complex too:

$$\mathbf{k} = k(1 - i\gamma) \quad (5)$$

generically, with  $k = \Re(\mathbf{k})$ . Specifically, the three groups of wavenumbers given by Eq. (4) become:

$$k_v = \pm k_v(1 - i\gamma_v) \quad (6a)$$

$$k_b = \pm k_b(1 - i\gamma_b) \quad \text{and} \quad k_b = \pm i k_b(1 - i\gamma_b) \quad (6b)$$

$$k_t = \pm k_t(1 - i\gamma_t) \quad (6c)$$

where these expressions are physical (waves attenuating along their direction of propagation) only if the generic coefficient  $\gamma$  defined above is positive. The second group of bending waves ( $k_b = \pm i k_b(1 - i\gamma_b)$ ) correspond to fast decaying and slowly oscillating waves.

Finally, Young and shear moduli can be identified from bending and twist wavenumbers composing the harmonic response of the beam. Considering the Euler model, the Young and shear moduli are given:

$$\mathbf{E}^{\text{eul}}(\omega) = \frac{M \omega^2}{I_b k_b^4} \quad \text{and} \quad \mathbf{G}(\omega) = \frac{J \omega^2}{I_t k_t^2} \quad (7)$$

The coefficients that are obtained are *apparent* Young and shear moduli, in the sense that they refer to an underlying theory of the Euler beam behaviour and not directly to elasticity. Consequently, they may vary in frequency.

## 2.2. The Timoshenko model

One can define one *equivalent slenderness ratio*  $\mu$  as the bending wavelength divided by the beam thickness:

$$\mu(\omega) = \frac{\lambda_b(\omega)}{h} = \frac{2\pi}{k_b(\omega)h} \quad (8)$$

When the frequency increases,  $\mu$  decreases. As a consequence, out-of-plane shear and rotary inertia effects are no longer negligible and the beam behaves as a thick beam. The Timoshenko model aims at taking into account these effects. The governing equation for bending motion in the harmonic regime (Eq. (2b)) can be found in [27]:

$$I_b E W'''' - \omega^2 M W + \omega^2 \rho I_b \left(1 + \frac{E}{\xi G}\right) W'' + \omega^4 \rho^2 \frac{I_b}{\xi G} = 0 \quad (9)$$

with  $\xi = \pi^2/12$  the shear correction factor. As in Eq. (4), the bending wave dispersion law is derived:

$$k_b^4 I_b E - \omega^2 M - \omega^2 k_b^2 \rho I_b \left(1 + \frac{E}{\xi G}\right) + \omega^4 \rho^2 \frac{I_b}{\xi G} = 0 \quad (10)$$

As in the preceding case, this fourth order equation in  $k$  gives four solutions, of which two are almost real and two are almost imaginary. Finally, an *apparent* Young modulus  $\mathbf{E}^{\text{tim}}$  that takes both out-of-plane shear effects and rotary inertia into account can be identified from the bending wavenumber  $k_b$  and the shear moduli  $\mathbf{G}(\omega)$  (Eq. (7)):

$$\mathbf{E}^{\text{tim}}(\omega) = \frac{\omega^2 M + \omega^2 k_b^2 \rho I_b - \omega^4 \rho^2 \frac{I_b}{\xi \mathbf{G}(\omega)}}{k_b^4 I_b - \omega^2 k_b^2 \rho \frac{I_b}{\xi \mathbf{G}(\omega)}} = \mathbf{E}^{\text{eul}}(\omega) \left( \frac{1}{1 - \frac{\omega^2 \rho}{k_b^2 \xi \mathbf{G}(\omega)}} + k_b^2 \frac{I_b}{A} \right) \quad (11)$$

The next section presents the signal model of a measurement performed on the beam, which parameters are identified by means of the proposed HRWA and of two existing methods suited for wavenumber identification: the *Mc Daniel method* [7] and the *Inhomogeneous Wave Correlation* [5].

## 3. Signal model

The harmonic response of a beam is measured on a domain away from sources and boundaries, along a regularly  $\Delta$ -spaced mesh  $\mathbf{x}$  of  $N$  points, aligned with the beam neutral axis:

$$x_u = x_1 + (u - 1)\Delta, \quad u \in \llbracket 1, N \rrbracket \quad (12)$$

A typical setup is schematised in Fig. 2.

For a beam structure vibrating in the linear regime, the measurement of a component of  $\mathbf{u}(x, y, z)$  along the mesh  $\mathbf{x}$  is expected to provide the spatially discrete signal  $\mathbf{s}$  formed by a sum  $\mathbf{p} = u_i(\mathbf{x}, y_0, z_0)$  of  $R$  damped exponentials and noise  $\mathbf{n}$  :

$$s_u = u_i(x_u, y_0, z_0) + n_u = p_u + n_u = \sum_{r=1}^R a_r z_r^u + n_u \quad (13)$$

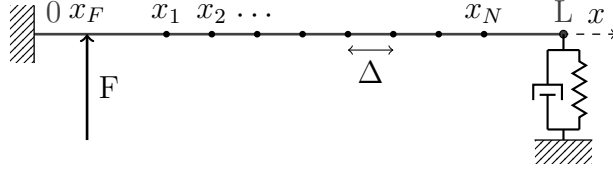


Figure 2: Typical setup for wavenumber identification methods.

where  $a_r$  are the amplitudes corresponding to the poles  $z_r = e^{ik_r\Delta}$ ,  $\mathbf{k}_r = k_r(1 - i \cdot \gamma_r)$ .

The  $\mathbf{p}$  part of the signal can be expressed as:

$$\mathbf{p} = \mathbf{V}_N(\mathbf{z}_R) \cdot \mathbf{a}_R \quad (14)$$

where  $\mathbf{a}_R = [a_1, \dots, a_R]^\top$ ,  $\mathbf{z}_R = [z_1, \dots, z_R]$  and  $\mathbf{V}_N(\mathbf{z}_R)$  is the Vandermonde matrix:

$$\mathbf{V}_N(\mathbf{z}_R) = \begin{bmatrix} 1 & \dots & 1 \\ z_1 & \dots & z_R \\ \vdots & \ddots & \vdots \\ z_1^{N-1} & \dots & z_R^{N-1} \end{bmatrix} \quad (15)$$

The main problem is to find the poles  $\mathbf{z}_R$ . Once the poles are known, the complex amplitudes  $\mathbf{a}_R$  can be estimated in the measured noisy signal  $\mathbf{s}$  in the least-square sense:

$$\mathbf{a}_R = (\mathbf{V}_N^*(\mathbf{z}_R) \cdot \mathbf{V}_N(\mathbf{z}_R))^{-1} (\mathbf{V}_N^*(\mathbf{z}_R) \cdot \mathbf{s}) \quad (16)$$

where  $\bullet^*$  denotes complex conjugate or hermitian transpose.

#### 4. Two existing wavenumber identification methods

As well as the HRWA method presented in this paper, the Mc Daniel and IWC methods make use of a Vandermonde matrix, but with different  $R$  and  $N$  values.

##### 4.1. One pole : Inverse Wave Correlation

The Inverse Wave Correlation method [5, 6] aims at finding the wavenumber  $\mathbf{k}$  which maximises the normalised scalar product  $C_{IWC}(\mathbf{k})$  between the Vandermonde vector  $\mathbf{v}_N(\mathbf{k}) = \mathbf{V}_N(e^{ik\Delta})$  and the noisy signal  $\mathbf{s}$ :

$$C_{IWC}(\mathbf{k}) = \frac{\mathbf{s} \cdot \mathbf{v}_N(\mathbf{k})}{\|\mathbf{s}\| \|\mathbf{v}_N(\mathbf{k})\|} \quad (17)$$

One can notice that the IWC correlation coefficient  $C_{IWC}(\mathbf{k})$  can be seen as a normalised  $z$ -transform on the complex wavenumber  $\mathbf{k}$ . Therefore, it suffers the same resolution limitations as any method based on a Fourier transform.

#### 4.2. Bending waves's four poles: the Mc Daniel method

Mc Daniel suggested [7, 8] to identify simultaneously the four waves derived from the bending operator (Eq. (2b), Eq. (3b) and Eq. (4b)). The four poles are imposed to be  $\mathbf{z}_4(\mathbf{k}) = [e^{ik\Delta}, e^{-ik\Delta}, e^{k\Delta}, e^{-k\Delta}]$ , where  $\mathbf{k}$  only has to be determined. A signal reconstruction  $\tilde{\mathbf{s}}(\mathbf{k})$  is made:

$$\tilde{\mathbf{s}}(\mathbf{k}) = \mathbf{V}_N(\mathbf{z}_4(\mathbf{k})) \cdot \mathbf{a}_4 \quad (18)$$

with the amplitudes  $\mathbf{a}_4$  estimated by Eq. (16). If only bending waves are present in the measured signal  $\mathbf{s}$ , its normalised correlation  $C_{\text{McDan}}(\mathbf{k})$  with the reconstructed signal  $\tilde{\mathbf{s}}(\mathbf{k})$ :

$$C_{\text{McDan}}(\mathbf{k}) = \frac{\mathbf{s} \cdot \tilde{\mathbf{s}}(\mathbf{k})}{\|\mathbf{s}\| \|\tilde{\mathbf{s}}(\mathbf{k})\|} \quad (19)$$

is maximum when  $\mathbf{k}$  matches the natural bending wavenumber.

Both methods are based on the maximisation of a correlation coefficient ( $C_{\text{IWC}}$  or  $C_{\text{McDan}}$ ). This is a non-linear problem on two unknowns: the real and imaginary parts of  $\mathbf{k}$ . For the comparisons given in the present paper, the procedure proposed by Rak [9] was adopted, using a Nelder-Simplex research algorithm.

### 5. High Resolution Wavenumber Analysis (HRWA) method: implementation for the characterisation of beams

The HRWA method makes use of the ESPRIT algorithm [22] (*Estimation of Signal Parameters via Rotational Invariance Techniques*) to extract wavenumbers from the harmonic response of a beam. It is inspired from the pioneer works of Prony [28], who stated that signals composed of complex poles follows a recurrence relation. This led, at the end of the twentieth century, to the development of a family of identification methods such as Matrix Pencil [29], Pisarenko method [30], MUSIC algorithm [31] and ESPRIT algorithm. The main goal of these methods consists in identifying, in a measured signal, complex poles with their associated amplitudes. These methods are widely used in array processing and radar applications [32, 33], musical applications [34, 15, 35] and high-resolution spectral analysis [36]. Some applications have been developed for the impact localisation on plates [37].

A Prony method has been already used in the past for the retrieval of dispersion relations in cylindrical shells [38][39]. However, it was limited by the sensibility to noise, the unknown number of travelling waves and the number of measurement points required to retrieve evanescent waves [40]. The ESPRIT algorithm, used here, applies subspace decomposition to improve the resistance to noise. In addition, the ESTER criterion [26] (*ESTimation or Error*) is used to estimate the *signal order* (number of poles contained in the signal). Finally, the procedure is here applied to full-field measurements, which allows to make measurement over fine meshes and overcome the limitations due to a limited number of points.

#### 5.1. The ESPRIT algorithm

##### 5.1.1. Signal and noise subspaces

The first step of the algorithm consists in the decomposition of the signal between signal and noise subspaces. First, a Hankel matrix  $\mathbf{H}$  is formed with the measured signal  $\mathbf{s}$  of

length  $N$ :

$$\mathbf{H} = \begin{bmatrix} s_1 & s_2 & \cdots & s_{N-K} \\ s_2 & s_3 & \cdots & s_{N-K+1} \\ \vdots & & \ddots & \vdots \\ s_K & \cdots & & s_N \end{bmatrix} \quad (20)$$

where the integer parameter  $K$  corresponds to the sum of the dimensions of signal and noise subspaces. The HRWA method makes use of the autocovariance matrix  $\mathbf{R}_{ss}$ :

$$\mathbf{R}_{ss} = \mathbf{H}\mathbf{H}^* = \mathbf{W}^* \mathbf{D} \mathbf{W} \quad (21)$$

which eigenvectors  $\mathbf{W}$  spans the same subspace as the Hankel matrix singular vectors, and has the advantage to be an asymptotically non-biased estimator of the signal autocovariance, in presence of white gaussian noise. The eigenvectors matrix  $\mathbf{W}$  spans the entire subspace of the noisy signal  $\mathbf{s}$ . This total subspace can be decomposed into signal subspace  $\mathbf{W}_p$  and noise subspace  $\mathbf{W}_n$ , with  $\mathbf{W}_p$  built with the eigenvectors corresponding to the  $R$  dominant eigenvalues (with the number of poles  $R$  supposed known here):

$$\mathbf{W} = \begin{bmatrix} [\mathbf{W}_p]_{K \times R} & [\mathbf{W}_n]_{K \times (K-R)} \end{bmatrix}_{K \times K} \quad (22)$$

It can be seen, with this last equation, that the parameter  $K$  has to be larger than  $R$ . Also, the dimension of the noise subspace is given by this parameter. In fact, the  $(K-R)$  additional poles contained in the noise subspace permits to sample an hypothetical correlated part of the noise [41], to separate it from the signal pole extraction. Numerous studies investigate this parameter influence on the errors of pole estimation [42, 43], and a common strategy consists in choosing this parameter so that  $K \approx N/2$ .

### 5.1.2. Rotational Invariance

Thanks to the regularity of the uniform measurement mesh  $\mathbf{x}$  of Eq. (12), a *rotational invariance* property is expressed via two Vandermonde matrices, related to two subparts of the signal:

$$\mathbf{V}_{(N-1)}^\downarrow(\mathbf{z}_R) = \mathbf{V}_{(N-1)}^\uparrow(\mathbf{z}_R) \cdot \mathbf{Z} \quad (23)$$

with  $\mathbf{Z} = \text{diag}(\mathbf{z}_R)$  and the two matrices  $\mathbf{V}_{(N-1)}^\uparrow$  and  $\mathbf{V}_{(N-1)}^\downarrow$  respectively corresponding to the  $(N-1)$  first and last samples of the signal. The ESPRIT algorithm strategy consists in estimating the signal poles  $\mathbf{z}_R$  via the signal subspace matrix  $\mathbf{W}_p$ . As this last matrix and the Vandermonde matrix spans close subspaces, they are related by a transfer matrix  $\mathbf{T}$ :  $\mathbf{V}_N(\mathbf{z}_R) = \mathbf{W}_p \mathbf{T}$ . The rotational invariance property is then expressed as a function of the signal subspace matrix:  $\mathbf{W}_p^\downarrow = \mathbf{W}_p^\uparrow \mathbf{F}$ , with  $\mathbf{F} = \mathbf{T} \mathbf{Z} \mathbf{T}^{-1}$  and:

$$\begin{aligned} \mathbf{W}_p^\uparrow &= \begin{bmatrix} \mathbf{I}_{(K-1)} & \mathbf{0}_{(K-1) \times 1} \end{bmatrix} \mathbf{W}_p \\ \mathbf{W}_p^\downarrow &= \begin{bmatrix} \mathbf{0}_{(K-1) \times 1} & \mathbf{I}_{(K-1)} \end{bmatrix} \mathbf{W}_p \end{aligned} \quad (24)$$

Consequently, the matrix  $\mathbf{F}$  is estimated in the Least-Square sense:

$$\mathbf{F} = (\mathbf{W}_p^\uparrow)^{-1} \mathbf{W}_p^\downarrow \quad (25)$$

Finally, the poles  $\mathbf{z}_R$  are extracted from the diagonalisation of  $\mathbf{F}$ .

### 5.1.3. Estimation of the number of poles

In the previous steps, the number of poles  $R$ , or *signal order*, has been supposed known. However, the number of dominant waves in the signal is unknown in most of the practical applications. As a wrong estimated signal order would drastically decrease the poles extraction accuracy, a signal order estimation method is needed. A number of signal order selection criterion have been proposed [44], as it is a common issue encountered in subspace-based identification methods. The HRWA method makes use of the ESTER criterion [26] (*ESTimation or ERror*), which is particularly adapted to the ESPRIT algorithm.

The estimation of matrix  $\mathbf{F}$  (Eq. (25)) is sensitive to the assumed signal order  $R$  used to extract the signal subspace (Eq. (22)). The ESTER criterion consists in finding the signal order  $R$  that minimises the  $\mathbf{F}$  estimation residual, so that :

$$R = \min_{r \in \llbracket r_{\min}, r_{\max} \rrbracket} \left\| \mathbf{W}_p^\uparrow(r) \mathbf{F}(r) - \mathbf{W}_p^\downarrow(r) \right\|_2 \quad (26)$$

With this criterion, the signal order  $R$  can be estimated automatically in a given range of signal orders  $r \in \llbracket r_{\min}, r_{\max} \rrbracket$ .

## 5.2. HRWA Implementation

For applying the HRWA to the characterisation of beams, any type of excitation may be used (impulse, random noise or sweep), with any type of actuator (e.g. shaker at  $x_F$ , exerting a point force  $F$  on the beam). The method has no requirement with regard to boundary conditions, provided that they are not applied too close to the measured zone. The displacement, velocity or acceleration  $\mathbf{S}(\mathbf{x}, \mathbf{t})$  is measured along a regularly spaced mesh  $\mathbf{x}$  of Eq. (12), as in Fig. 2. A collection of harmonic responses is obtained by computing the Fourier Transform  $\mathbf{S}(\mathbf{x}, \boldsymbol{\omega})$  of the measured signal over the time dimension for a given number of individual frequencies  $\omega_i$ . The HRWA procedure consists in applying the following steps to each obtained harmonic response  $\mathbf{s}(\omega_i) = \mathbf{S}(\mathbf{x}, \omega_i)$ :

1. A Hankel matrix  $\mathbf{H}$  is built, based on the array  $\mathbf{s}(\omega_i)$  (see Eq. (20)).
2. The Covariance Matrix  $\mathbf{R}_{ss}$  is computed and diagonalised yielding the matrix of eigenvectors  $\mathbf{W}$  (see Eq. (21)).
3. The ESTER method is applied to estimate the signal order, in other words the number of detectable waves in the (noisy) signal. Then, for each  $r \in \llbracket r_{\min}, r_{\max} \rrbracket$  :
  - (a) the  $r$  eigenvectors corresponding to the  $r$  dominant eigenvalues are extracted to form the approximated signal subspace matrix  $\mathbf{W}_p$  (Eq. (22))
  - (b) the truncated signal subspace matrices  $\mathbf{W}_p^\uparrow$  and  $\mathbf{W}_p^\downarrow$  are built (Eq. (24))
  - (c) the Least-Squares estimation of  $\mathbf{F}$  is computed (Eq. (25))
  - (d) the ESTER criterion as function of  $r$  is evaluated (Eq. (26))

Finally, the signal order  $R$  is chosen to minimise the ESTER criterion.

4. The eigenvalues of the matrix  $\mathbf{F}$  (see Eq. (25)) are computed, yielding the wavenumbers  $\mathbf{k}_r$  of all the waves which can be detected with the HRWA at the angular frequency  $\omega_i$ :

$$\mathbf{k}_r(\omega_i) = \frac{\ln(i \cdot z_r(\omega_i))}{\Delta} \quad (27)$$

5. If a signal reconstruction is needed, the Vandermonde matrix  $\mathbf{V}_N(\mathbf{z}_R)$  is computed (Eq. (15)), and the complex amplitudes  $\mathbf{a}_R$  are estimated (Eq. (16)).

## 6. Comparison of methods for a simulated cantilever bending-only beam

This section is devoted to a comparison between the Mc Daniel method, the IWC method and the HRWA, regarding the sensitivity to noise and the computation time. For this purpose, a simple case is investigated numerically. Using synthesised data for the comparison makes possible the exploration of various parameters (e.g. mesh size, material characteristics, etc.). A thin aluminium cantilever Euler beam of length  $L$  is harmonically excited at the pulsation  $\omega$  with a force  $F = 1N$  at  $(x_F, y_F, z_F) = (L, 0, h/2)$  (Fig. 3), in order to be submitted to bending only. In this situation, the signal model of the Mc Daniel method is exact: the harmonic response of the beam is composed of four bending waves, with wavenumbers  $k_b$  solutions of the fourth root of Eq. (4b). It is thus the reference method for this case study.

The characteristics of the beam are summarised in Tab. 1. The beam is excited between 10 Hz and 5 kHz. Eleven resonance peaks appear in this bandwidth (see Fig. 4, top frame). The first modal frequency is around 14 Hz.

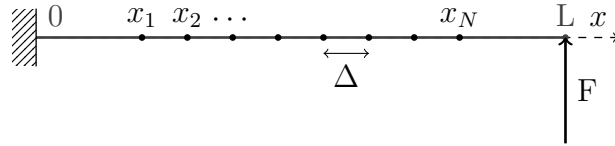


Figure 3: The simulated cantilever beam.

The response of the beam is derived analytically since the four complex amplitudes  $w_j$  in Eq. (3) are determined by the boundary conditions. The response yields the virtual measurements on the mesh  $\mathbf{x}$  of Eq. (12) along a sub-part of the beam ( $x_u \in [0.1, 0.9] \times L$ ). The beam response is computed at 100 equally-spaced frequencies in the desired bandwidth, and for 100 regularly spaced points over the sub-part of the beam.

$L$	$h$	$b$	$E$	$\eta$	$\nu$	$\rho$
60 cm	6 mm	40 mm	70 GPa	0.5%	0.3	2500

Table 1: Characteristics of the beam.

### 6.1. Noise Sensitivity

To study the sensitivity to noise of each wavenumber identification method, a white gaussian noise is added to the signal  $\mathbf{s}$ . The amplitude of this noise is determined by a given Signal to Noise Ratio (SNR). For each of the 100 SNR values ranging from  $10^0$  to  $10^4$  and each of the 100 computed beam harmonic responses, 100 realisations of the noisy signal are computed. Altogether, the estimation of the bending wavenumber is done one million times for each method. Based on these 100 realisations of the noise the mean and variance of the wavenumber estimation error are computed, as a function of frequency and SNR.

The Mc Daniel method and IWC method identify only one wavenumber  $k$ . By contrast, the HRWA identifies a varying number of wavenumbers. Consequently a *valid wavenumber*

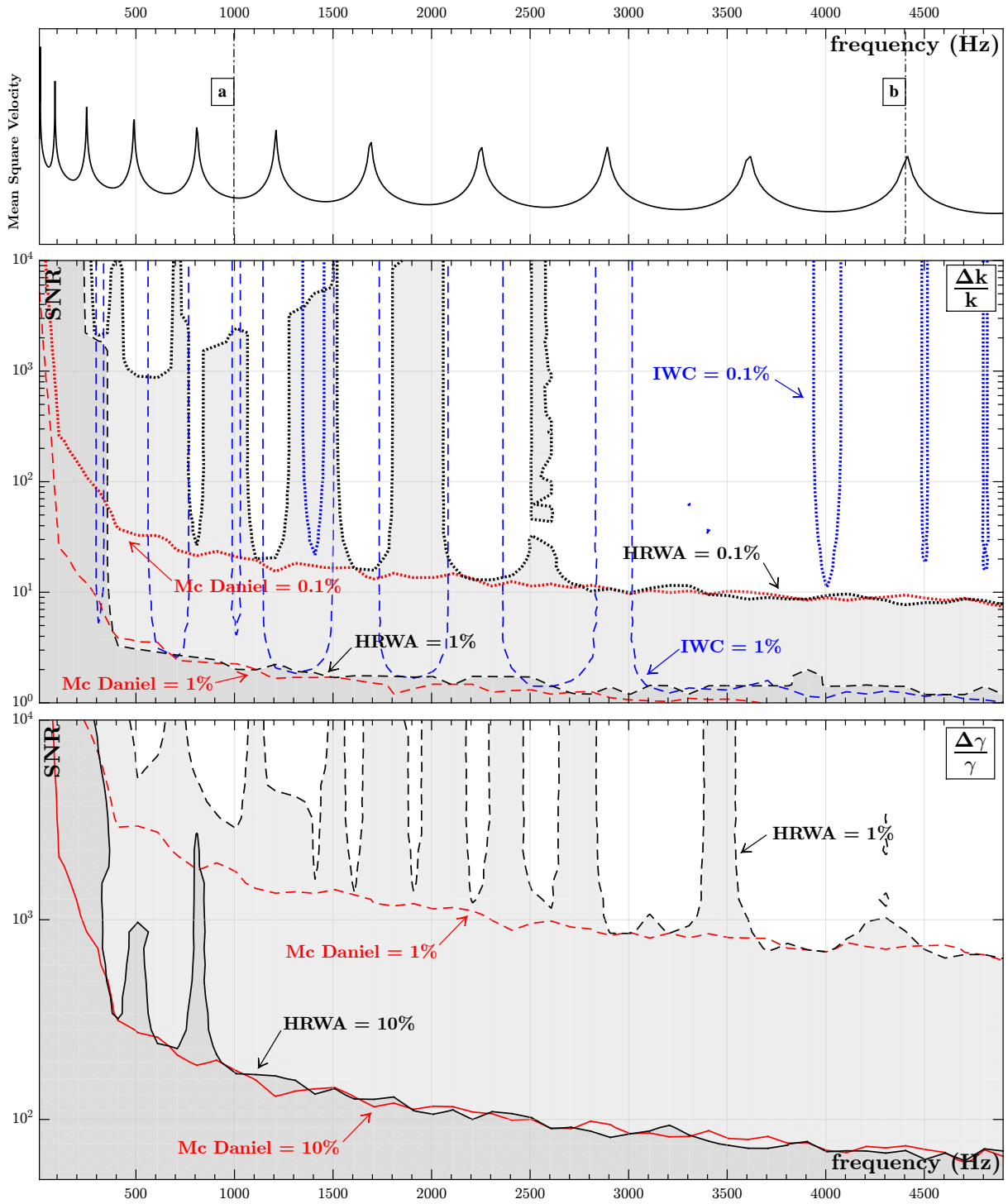
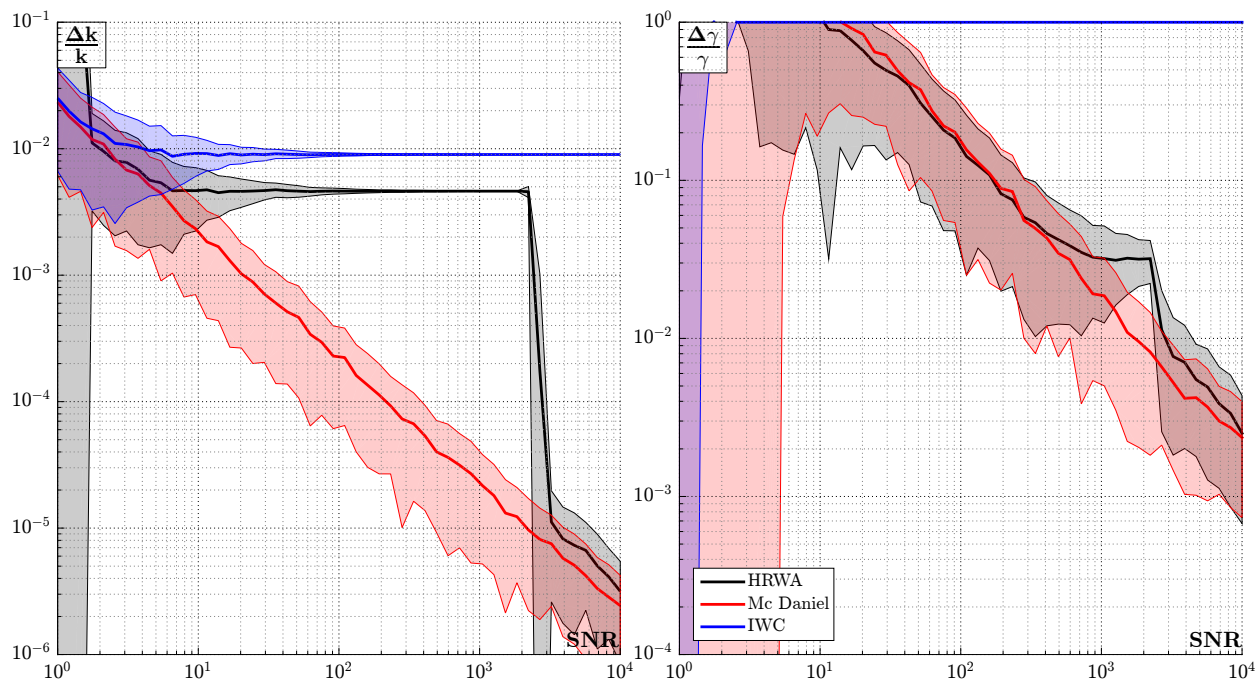
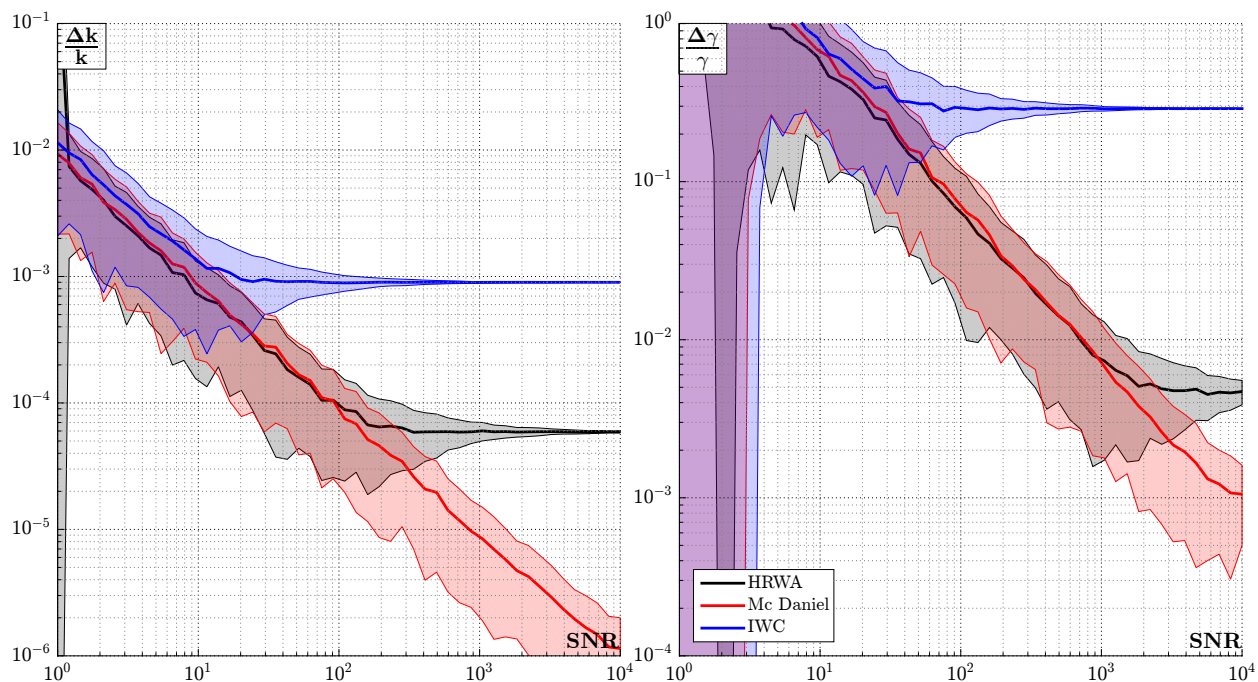


Figure 4: Synthesised Mean Square Velocity without noise (top frame). Contour plots of the relative errors in the determination of the real part of the wavenumber  $k$  (middle frame) and the spatial decay  $\gamma$  (bottom frame) for different SNR levels (ordinates) as a function of the frequency. Comparison of the HRWA (black), Mc Daniel (red) and IWC (blue) methods. Contour lines display the 10% (continuous lines), 1% (dashed lines) and 0.1% (dotted lines) limits for the relative identification errors. The results are obtained as the mean of the estimation over 100 virtual tests.



(a) 1000 Hz, between two modal frequencies



(b) 4400 Hz, on a modal frequency

Figure 5: Relative error in the identification of the complex wavenumber  $k = k(1 - i \cdot \gamma)$  as a function of the SNR for two fixed frequencies. Mean  $\pm$  Standard Deviation. Comparison between HRWA (black), Mc Daniel (red) and IWC (blue) methods. (a) at 1 kHz, between two modal frequencies. (b) at 4.5 kHz, on a modal frequency.

*selection strategy* has to be chosen to perform the comparison. All along this numerical investigation, the maximum signal order  $r_{\max}$  of the HRWA procedure is given by the equilibrium (Eq. (3)). The algorithm is then free to identify from one to eight waves of different wavenumbers ( $R \in \llbracket 1, 8 \rrbracket$ ). The choice is automated with the ESTER criterion. The chosen strategy, which was observed to work the best among several options, consists in isolating the  $P$  *propagative* wavenumbers  $\mathbf{k}_p$  so that  $0 < \gamma_p < 1$ . The mean of these wavenumbers is then computed as follows:

$$\mathbf{k} = \frac{1}{P} \left( \sqrt{\sum_{p=1}^P \operatorname{Re}(\mathbf{k}_p)^2} - i \sqrt{\sum_{p=1}^P \operatorname{Im}(\mathbf{k}_p)^2} \right) \quad (28)$$

the square power allowing to take into account both *forward* and *backward* propagating waves. This strategy eliminates the identified *evanescent* (fast decreasing) waves, the identification of which is sensitive to noise.

In Fig. 4 and Fig. 5, average relative errors on the identification of the real part  $k$  of the wavenumber and the spatial decay  $\gamma$  are represented for the IWC method, the Mc Daniel method and the HRWA. In Fig. 4, three contour lines are plotted, corresponding on three levels of performance (relative error of 10%, 1% and 0.1%). The wavenumber identification turns out to be sensitive to the number of spatial periods contained in the measurement mesh. As the wavelength depends on frequency, it has been chosen to represent the relative error on the complex bending wavenumber estimation as a function of frequency and of Signal to Noise Ratio.

Regarding the real part of the bending wavenumber, both HRWA and Mc Daniel method give an estimation with less than 1% of relative error, above 500 Hz and for small signal to noise ratios ( $\text{SNR} > 3$ ). The Mc Daniel method provides a relative error of 0.1% in the estimation, up to a  $10^2$  SNR, whereas the HRWA delivers such an estimation above 3kHz. The HRWA and the Mc Daniel methods display comparable abilities to provide an estimation of the spatial decay with less than 10% of relative error. For high signal to noise ratios ( $\text{SNR} > 10^3$ ), the Mc Daniel method can give an estimation of the spatial decay with less than 1% of relative error, above 2.5 kHz, whereas this frequency bound is higher for the HRWA (4kHz).

In contrast, the estimate of the IWC method depends on the frequency. This behaviour is related to its resolution limitations. Except for few high frequencies, no estimation of the real part of the wavenumber with IWC can be made with less than 0.1% of relative error. Moreover, the estimation of the spatial decay  $\gamma$  is not possible to the IWC method in this SNR and frequency ranges. These results agree with those of Rak [9].

The HRWA method exhibits a frequency-dependent behaviour for the fine estimation of real part of wavenumber (0.1% of relative error) and spatial decay (1% of relative error): both real and imaginary parts of the wavenumber are better identified at modal frequencies. In order to explain this particular behaviour, results of the study for two given frequencies are plotted in Fig. 5. It shows the results of complex bending wavenumber identification as a function of SNR, for the three methods. First, Fig. 5a shows the results at 1000 Hz, between two modal frequencies (see Fig. 4, top frame, marker  $\boxed{\text{a}}$ ). For this particular frequency, the

HRWA converges shortly to a first plateau at 0.5% of relative error in  $k$  identification, for SNR higher than  $10^1$ . Then, one can observe a jump at SNR of 2000, HRWA finally reaching a very fine estimation of the real part  $k$  of the wavenumber, comparable to the Mc Daniel method. The level and the extension of the plateau are due to the variable estimation of the number of waves in the signal by the ESTER criterion, an effect which appears to be stronger between modal frequencies. The spatial decay estimation is affected by this plateau effect too, the relative error converging to a value of 3%, below a SNR of 2000. By comparison, the error of the estimation of  $k$  with the IWC method reaches a plateau too, which is higher (0.9% of relative error) and related to its resolution limitation. Furthermore, the Mc Daniel method shows a uniform convergence rate, with a relative error fifty times smaller than the noise ratio on  $k$  ( $\Delta k/k \approx (50 \text{ SNR})^{-1}$ ) and twenty times larger on the spatial decay ( $\Delta \gamma/\gamma \approx 20 (\text{SNR})^{-1}$ ). In Fig. 5b, the same data has been plotted, but for a higher frequency of 4400Hz which coincides with a modal frequency (see Fig. 4, top frame, marker b), where the three methods provides a *good* estimation of the real part of the wavenumber. Here, the plateau reached by the HRWA error is much lower ( $\approx 6 \times 10^{-5}$  of relative error) than in the previous case. The HRWA, before this plateau, shows the same convergence rate as Mc Daniel method, both for  $k$  and  $\gamma$  estimation. It has to be noted that IWC method, in this case, estimates the spatial decay with approximately 15% of relative error.

The plateau effect of HRWA shown previously is due to the possibility given to the ESPRIT algorithm, to select the number of waves in the signal (thanks to the ESTER criterion), and by making no assumption on a relation between each wavenumber. This is the main difference with Mc Daniel method's signal model, which confers to this last method its stability against the noise level, when only bending waves are present. However, this plateau appears below 1% of relative error on the real part of the wavenumber and 10% of relative error on the spatial decay, which is are good estimations, altogether.

## 6.2. Comparison of Computation Times

In addition to noise sensitivity, the computation time of each method has been investigated. As these methods extract wavenumbers from one single frequency component, the computation time is independent from frequency. It is only dependent on the size  $N$  of the measurement mesh. From 10 to 1000 measurement points have been exported from the synthesised forced response's shape. The computation time has been averaged on 20 frequency points and 10 iterations. The results of the study are plotted in Fig. 6.

This figure illustrates the advantages of HRWA in terms of computational cost: it is, depending on the mesh size, five to twenty times faster than the two other methods. This makes wavenumber analysis suitable for real-time applications, such as structural health monitoring. The computational cost of Mc Daniel and IWC methods is mainly caused by the amount of iterations needed in the two dimensional non-convex minimisation problem in  $k$ .

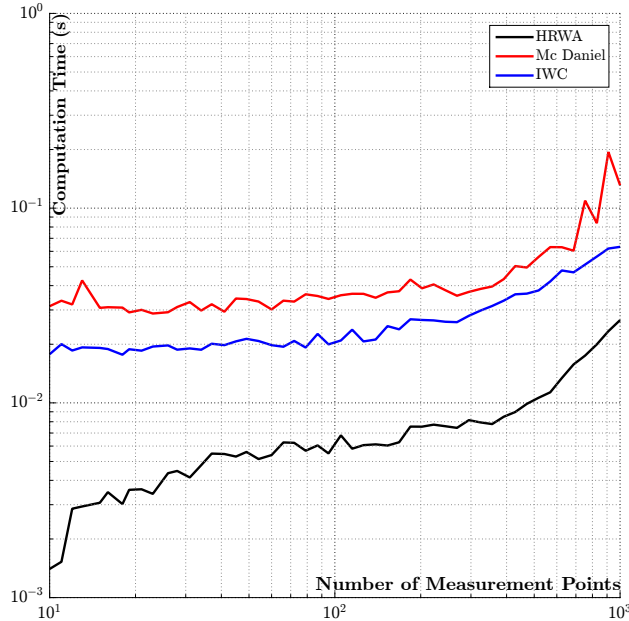


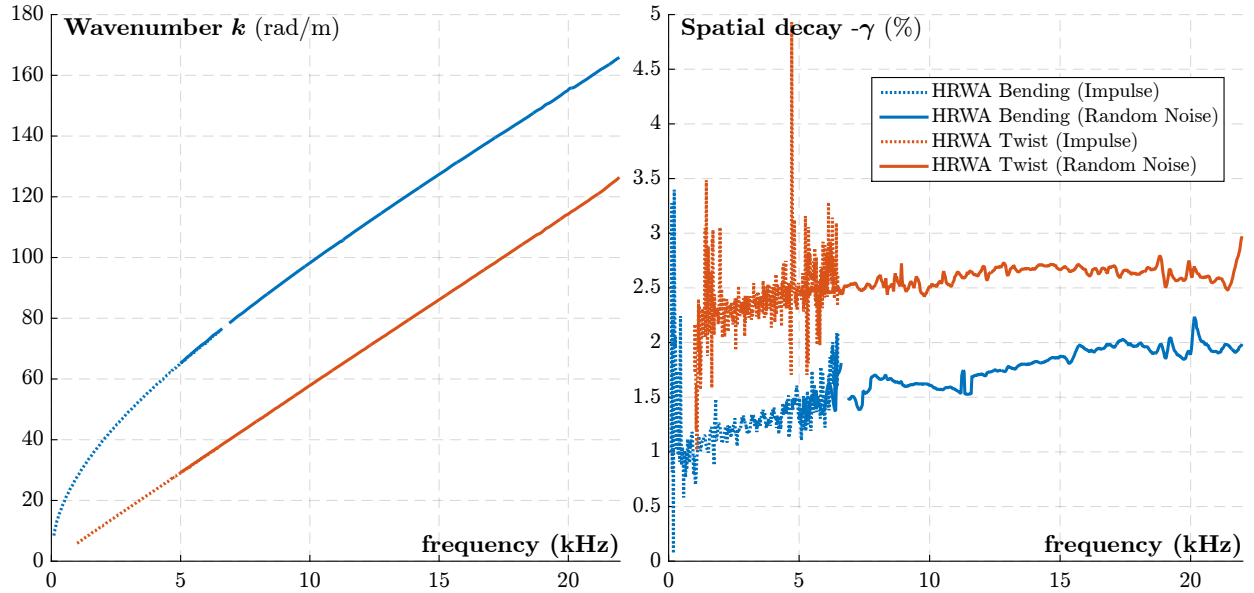
Figure 6: Computation time of each wavenumber identification method as a function of the measurement mesh size, averaged on 200 wavenumbers extractions. Comparison between methods.

## 7. Experimental Results

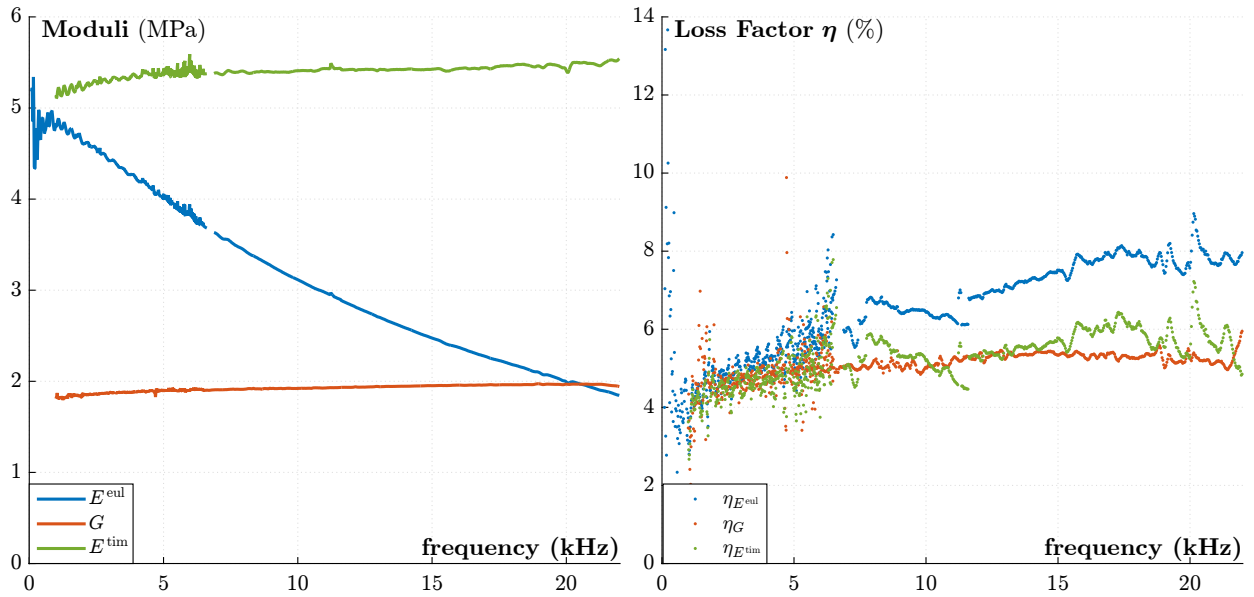
An experimental application is performed on a simple rigid PVC (polyvinyl chloride) beam. The beam’s section is square of side 15mm, and its length of 1m. The velocity is measured with a Doppler laser vibrometer along a regular mesh of 500 points over the top surface of the beam. Consequently, the mesh is shifted from the beam neutral axis ( $y \neq 0$  in Eq. (1)). Hence both bending and twist motion contributes in the measured velocity. A shaker is fixed at one end of the beam ( $(x_F, y_F, z_F) = (0, -b/2, -h/2)$ , see Fig. 1), whereas the other end is supported by a silicon block.

A first measurement is performed with an impulse excitation, achieved by sending an electrical pulse to the shaker. A second measurement is made with a random noise excitation filtered between 5 kHz and 22 kHz. In both cases, the frequency response is estimated from the average of 20 realisations, respectively below 6 kHz and between 5 and 22 kHz. For both experiments, a sampling frequency of 50 kHz was used.

The HRWA is applied to the computed frequency transfer estimator  $H1$  between the measured velocity and the electrical excitation signal (no force measurement). As the measurement mesh is shifted from the neutral axis, it contains both the bending and twist motion’s contributions. Fig. 7a shows the HRWA results, for both excitation type. It shows that the HRWA is able to identify both bending (blue) and twist (red) wavenumbers, at each frequency. It can be observed that both the real and imaginary parts of the identified wavenumbers are independent of the excitation type: the wavenumbers extracted in the overlapping frequency band (between 5Hz and 6kHz) are identical. By combining different excitations, a wavenumber extraction can be achieved in a very wide frequency domain. The



(a)



(b)

Figure 7: Experimental application of the HRWA to a PVC beam of length  $L = 1$  m and square section of side  $h = b = 15$  mm, for frequencies between 0 and 22 kHz. (a) Identification of wavenumbers on the measured beam with the proposed HRWA, for two excitation types: impulse (dashed lines) and steady noise (solid line). Bending wavenumber  $k_b$  (blue) and twist wavenumber  $k_t$  (red). (b) Apparent complex moduli identification from the extracted wavenumbers: With the Euler model ( $E^{\text{eul}}$  (blue) and  $G$  (red) from Eqs. (7)) and the Timoshenko model ( $E^{\text{tim}}$  (green) from Eq. (11)).

minimum identified wavelength  $\lambda = 2\pi/k$  is approximately 3.7 cm, which means that at least 18 measurement points are contained in each wavelength. Following the Nyquist criterion, a coarser measurement mesh could have been taken ( $\approx 8$  times less points). However, taking a finer mesh improves the identification accuracy, as the parameter identification is made in the least-square sense (Eq. (25)).

Observing the wavenumber dependence as a function of frequency, two dispersion branches can be built, related to the bending and to the twist motions. Within the frame of the Euler beam theory, one can connect wavenumbers to the Young and shear moduli according to Eq. (7). The results of the identification of the *apparent* Young modulus  $E^{\text{eul}}$  (in blue, from bending branch) and shear modulus  $G$  (in red, from twist branch) are shown in Fig. 7b (with  $\kappa = 0.845$  for a square section and the PVC density  $\rho = 1380 \text{ kg/m}^3$ ). The low-frequency estimation is noisier because of the plateau effects of the HRWA related to the modal behaviour of the beam (see preceding section). As the frequency increases, the beam's response tends to be smoother and the number of spatial periods increases, leading to a better wavenumber estimation.

The dependency on frequency of the identified complex apparent Young modulus  $E^{\text{eul}}$  is mainly due to the transverse shear effects generated by the bending motion, that increases with the frequency. To explain these effects, one can use the equivalent slenderness ratio defined in Eq. (8). At low frequencies, this ratio is large ( $\mu(100 \text{ Hz}) \simeq 42$ ) and the beam behaves as a thin beam. As the frequency increases,  $\mu$  decreases ( $\mu(5 \text{ kHz}) \simeq 6.5$ ,  $\mu(20 \text{ kHz}) \simeq 2.7$ ) and the beam behaves as a thick beam. In order to take these effects into account, the Timoshenko model is used to better estimate the Young modulus. By injecting the identified shear modulus  $G$  in the equation (11) leads to the estimation of an other Young modulus,  $E^{\text{tim}}$  (in green). The result is shown on Fig. 7b in yellow. It can be observed that the identified modulus is almost constant ( $\simeq 5.5 \text{ GPa}$ ) in the considered frequency range. The resulting Poisson ratio is estimated as  $\nu = E/(2G) - 1 \simeq 0.4$ . In addition, the identified Young loss factor  $\eta_{E^{\text{tim}}}$  seems very close to the shear loss factor  $\eta_G$ .

## 8. Conclusion and Perspectives

A common framework for wavenumber extraction methods has been presented and the *High Resolution Wavenumber Analysis* has been proposed. This new method aims at overcoming three following drawbacks of the IWC and the Mc Daniel methods: (a) IWC suffers from resolution limitations (b) the nonlinear wavenumber search problem is computationally heavy and (c) the number of identified waves is fixed and small.

The HRWA procedure includes a linear search of wavenumbers. Thus, the computation cost is reduced and the wavenumber identification is free from any initialisation. Moreover, it allows an automated determination of wavenumbers in a noisy signal without *a priori* assumption on their number. The detected waves are not limited to bending waves but can be associated with twist, compression, shear, etc.

Firstly, numerical investigations and comparisons of HRWA with the two other methods has been led in simple cases, including that of a thin prismatic Euler beam. When only bending waves are present, the *Mc Daniel method* can be taken as a reference method.

In this simple case, this method is the least sensitive to noise. The IWC method fails to identify a spatial decay, in the frequency band studied. The HRWA exhibits a convergence rate as function of the signal to noise ratio comparable to the Mc Daniel method ( $\Delta k/k \approx 0.02 \text{ SNR}^{-1}$ ), with certain fluctuations for a very precise determination of the real part of the wavenumber (0.1% of relative error). These fluctuations are mainly due to the fact that the method has no *a priori* assumptions with regard to the number of wavenumbers present in the signal, as opposed to the Mc Daniel method. The spatial decay has a reduced influence on the measured beam harmonic response, compared to the real part of the wavenumber. Therefore, its determination is more sensitive to noise. An estimation with a relative error of 10% can be achieved with both Mc Daniel and HRWA methods, for good signal to noise ratios ( $\text{SNR} > 100$ ). Moreover, the comparison of computational times shows that HRWA can be twenty times faster than the two other methods.

Secondly, the HRWA has been applied to experimental data. It emphasises the ability of the HRWA to simultaneously identify apparent complex Young and shear modulus, as a function of frequency, independently from boundary conditions or excitation type. Identified with the Euler model, the Young modulus vary in frequency. To account for the out-of-plane shear and rotary inertia effects, the Timoshenko model is finally used and leads to the identification of a Young modulus which is almost constant in the frequency range of interest.

It has been observed that most of the identification errors of the HRWA results are related to a wrong signal order estimation. Indeed, the ESTER criterion performs well only if the signal model is correct. In order to improve the robustness of the HRWA, other signal order selection criterion could be investigated. For example, the use of a stabilisation diagram [45, 46] to estimate the order of the signal could improve the accuracy of the wavenumber estimation, at the price of a reasonable increase of the computational burden.

At this point, it appears clearly that no hypothesis has been made on the nature of the waves: the HRWA is not limited to the simple beam models presented here. For example, a different section or material configuration may induce coupled strain mechanisms and coupling the characteristic in equations (2) and (3). The detected wavenumbers would be different, but still be representative of the structural behaviour, reasonably far from the boundary conditions.

The present paper is focused on material characterisation but the HRWA can also be used for the identification of boundary conditions (not presented here). Moreover, multidimensional versions of ESPRIT [33] and ESTER [47] have been developed and can be applied to the experimental identification of wavevectors in the harmonic response of plates. This will be the object of a forthcoming paper.

## Acknowledgments

This work is part of the ANR founded (french National Research Agency) project MAESSTRO (*Modélisation Et Synthèse Sonore pour Tables d'harmonie de piano*, ANR-14-CE07-0014). The authors thank Kerem Ege for his precious help on high-resolution signal processing methods.

## References

- [1] S. Avril, M. Bonnet, A. S. Bretelle, M. Grédiac, F. Hild, P. Ienny, F. Latourte, D. Lemosse, S. Pagano, E. Pagnacco, F. Pierron, Overview of identification methods of mechanical parameters based on full-field measurements, *Experimental Mechanics* 48 (4) (2008) 381–402.
- [2] C. Pezerat, J. L. Guyader, Identification of vibration sources, *Applied Acoustics* 61 (3) (2000) 309–324.
- [3] Q. Leclère, C. Pézerat, Vibration source identification using corrected finite difference schemes, *Journal of Sound and Vibration* 331 (6) (2012) 1366–1377.
- [4] T. Wassereau, C. Pezerat, J.-L. Guyader, F. Ablitzer, Characterization of materials and flaw detection using force analysis technique, in: *NOVEM 2015*, no. April, Dubrovnik, Croatia, 2015.
- [5] J. Berthaut, Contribution à l'identification large bande des structures anisotropes. {Contribution to the wide-band identification of anisotropic structures.}, Ph.D. thesis, École Centrale de Lyon (2004).
- [6] J. Berthaut, M. N. Ichchou, L. Jezequel, K-space identification of apparent structural behaviour, *Journal of Sound and Vibration* 280 (2005) 1125–1131.
- [7] J. G. McDaniel, W. S. Shepard Jr., Estimation of structural wave parameters from spatially sparse response measurements, *Journal of the Acoustical Society of America* 108 (4) (2000) 1674–1682.
- [8] V. Palan, W. S. Shepard, J. G. McDaniel, Characterization of an experimental wavenumber fitting method for loss factor estimation using a viscoelastically damped structure, *Journal of Sound and Vibration* 291 (3-5) (2006) 1170–1185.
- [9] M. Rak, M. Ichchou, J. Holnicki-Szulc, Identification of structural loss factor from spatially distributed measurements on beams with viscoelastic layer, *Journal of Sound and Vibration* 310 (4-5) (2008) 801–811.
- [10] H. Oberst, K. Frankenfeld, Über die dämpfung der biegeschwingungen dünner bleche durch fest haftende beläge. {On the damping of bending vibrations of thin sheets by adherent coverings.}, *Acta Acustica united with Acustica* 2 (6) (1952) 181–194.
- [11] H. Oberst, G. W. Becker, K. Frankenfeld, Über die dämpfung der biegeschwingungen dünner bleche durch fest haftende beläge II. {On the damping of bending vibrations of thin sheets by adherent coverings II.}, *Acta Acustica united with Acustica* 4 (4) (1954) 433–444.
- [12] J.-M. Berthelot, Y. Sefrani, Damping analysis of unidirectional glass and Kevlar fibre composites, *Composites Science and Technology* 64 (9) (2004) 1261–1278.
- [13] J.-M. Berthelot, Damping analysis of laminated beams and plates using the Ritz method, *Composite Structures* 74 (2) (2006) 186–201.
- [14] J.-M. Berthelot, M. Assarar, Y. Sefrani, A. E. Mahi, Damping analysis of composite materials and structures, *Composite Structures* 85 (3) (2008) 189–204.
- [15] K. Ege, X. Boutillon, B. David, High-resolution modal analysis, *Journal of Sound and Vibration* 325 (4-5) (2009) 852–869.
- [16] M. Rébillat, X. Boutillon, Measurement of relevant elastic and damping material properties in sandwich thick plates, *Journal of Sound and Vibration* 330 (25) (2011) 6098–6121.
- [17] L. Jaouen, A. Renault, M. Deverge, Elastic and damping characterizations of acoustical porous materials: Available experimental methods and applications to a melamine foam, *Applied Acoustics* 69 (12) (2008) 1129–1140.
- [18] B. Hosten, M. Deschamps, Inhomogeneous wave generation and propagation in lossy anisotropic solids. Application to the characterization of viscoelastic composite materials, *Journal of Acoustical Society of America* 82 (5) (1987) 1763–1770.
- [19] B. Audoin, C. Bescond, M. Deschamps, Measurement of stiffness coefficients of anisotropic materials from pointlike generation and detection of acoustic waves, *Journal of Applied Physics* 80 (1996) (1996) 3760–3771.
- [20] M. Kersemans, A. Martens, K. Van Den Abeele, J. Degrieck, L. Pyl, F. Zastavnik, H. Sol, W. Van Paepegem, The quasi-harmonic ultrasonic polar scan for material characterization: Experiment and numerical modeling, *Ultrasonics* 58 (2015) 111–122.
- [21] D. Duhamel, B. R. Mace, M. J. Brennan, Finite element analysis of the vibrations of waveguides and periodic structures, *Journal of Sound and Vibration* 294 (1-2) (2006) 205–220.

- [22] R. Roy, T. Kailath, ESPRIT-Estimation of Signal Parameters via Rotational Invariance Techniques, *IEEE Transactions on Acoustics, Speech, and Signal Processing* 37 (7) (1989) 984–995.
- [23] B. L. Ho, R. E. Kalman, Effective construction of linear state-variable models from input/output functions 1), at - *Automatisierungstechnik* 14 (1-12) (1966) 545–548.
- [24] P. Van Overschee, B. L. De Moor, *Subspace identification for linear systems: Theory—Implementation—Applications*, Springer Science & Business Media, 2012.
- [25] J.-n. Juang, R. S. Pappa, An Eigensystem Realization Algorithm for Modal Parameter Identification and Model Reduction, *Journal of guidance, control, and dynamics* 8 (5) (1985) 620–627.
- [26] R. Badeau, B. David, G. Richard, A new perturbation analysis for signal enumeration in rotational invariance techniques, *IEEE Transactions on Signal Processing* 54 (2) (2006) 450–458.
- [27] A. Bhaskar, Elastic waves in Timoshenko beams: the ‘lost and found’ of an eigenmode, *Proceedings of the Royal Society A: Mathematical, Physical and Engineering Sciences* 465 (2101) (2009) 239–255.
- [28] R. Prony, Essai experimental et analytique. {experimental and analytical assay.}, *Journal de l’École Polytechnique* 1 (22) (1795) 24–76.
- [29] Y. Hua, T. K. Sarkar, Matrix Pencil Method for Estimating Parameters of Exponentially Damped/Undamped Sinusoids in Noise, *IEEE Transactions on Acoustics, Speech, and Signal Processing* 38 (5) (1990) 814–824.
- [30] V. F. Pisarenko, The Retrieval of Harmonies from a Covariance Function, *Geophysical Journal of the Royal astrophysical Society* 33 (1973) 347–366.
- [31] R. Schmidt, *A Signal Subspace Approach to Multiple Emitter Location and Spectral Estimation*, Ph.D. thesis, Stanford University (1981).
- [32] S. Shahbazpanahi, S. Valaee, M. H. Bastani, Distributed source localization using ESPRIT algorithm, *IEEE Transactions on Signal Processing* 49 (10) (2001) 2169–2178.
- [33] S. Rouquette, M. Najim, Estimation of frequencies and damping factors by two-dimensional ESPRIT type methods, *IEEE Transactions on Signal Processing* 49 (1) (2001) 237–245.
- [34] V. Emiya, B. David, R. Badeau, A parametric method for pitch estimation of piano tones, *ICASSP, IEEE International Conference on Acoustics, Speech and Signal Processing - Proceedings* 1.
- [35] R. Badeau, B. David, R. Boyer, Eds *Parametric Modeling And Tracking Of Audio Signals*, *Proceedings of 5th Int. conf. on Digital Audio Effects (DAFx02)* (2002) 26–28.
- [36] R. Badeau, B. David, G. Richard, High-resolution spectral analysis of mixtures of complex exponentials modulated by polynomials, *IEEE Transactions on Signal Processing* 54 (4) (2006) 1341–1350.
- [37] L. Qiu, B. Liu, S. Yuan, Z. Su, Impact imaging of aircraft composite structure based on a model-independent spatial-wavenumber filter, *Ultrasonics* 64 (2016) 10–24.
- [38] T. J. Plona, B. K. Sinha, S. Kostek, S.-k. Chang, Axisymmetric wave propagation in fluid-loaded cylindrical shells. II: Theory versus experiment, *Journal of the Acoustical Society of America* 92 (August) (1992) 1144–1155.
- [39] J. Vollmann, R. Brey, J. Dual, High-resolution analysis of the complex wave spectrum in a cylindrical shell containing a viscoelastic medium .2. Experimental results versus theory, *Journal Of The Acoustical Society Of America* 102 (2) (1997) 909–920.
- [40] K. Grosh, E. G. Williams, Complex wave-number decomposition of structural vibrations, *The Journal of the Acoustical Society of America* 93 (2) (1993) 836–848.
- [41] R. Kumaresan, D. Tufts, Estimating the parameters of exponentially damped sinusoids and pole-zero modeling in noise, *Acoustics, Speech and Signal Processing, IEEE Transactions on* 30 (6) (1982) 833–840.
- [42] J. Laroche, The use of the matrix pencil method for the spectrum analysis of musical signals, *The Journal of the Acoustical Society of America* 94 (4) (1993) 1958–1965.
- [43] R. Badeau, *Méthodes à haute résolution pour l’estimation et le suivi de sinusoïdes modulées. application aux signaux de musique* {High-resolution methods for the estimation and the tracking of modulated sinusoids. Application to musical signals.}, Ph.D. thesis, Télécom ParisTech (2005).
- [44] P. Stoica, Y. Sel, Model-Order Selection: A review of information criterion rules, *IEEE Signal processing Magazine* 21 (July) (2004) 36–47.

- [45] P. G. Bakir, Automation of the stabilization diagrams for subspace based system identification, *Expert Systems With Applications* 38 (12) (2011) 14390–14397.
- [46] E. Reynders, J. Houbrechts, G. D. Roeck, Fully automated (operational) modal analysis, *Mechanical Systems and Signal Processing* 29 (2012) 228–250.
- [47] K. Liu, J. P. C. da Costa, H. Cheung So, L. Huang, Subspace techniques for multidimensional model order selection in colored noise, *Signal Processing* 93 (2013) 1976–1987.